

# BER Performance Analysis of MIMO Systems Using Equalization Techniques

Rohit Gupta<sup>1</sup>, Amit Grover<sup>2\*</sup>

1. Department of Electronics and Communication Engineering, Shaheed Bhagat Singh State Technical Campus, Moga Road (NH-95), Ferozepur-152004, India.
2. Department of Electronics and Communication Engineering, Shaheed Bhagat Singh State Technical Campus, Moga Road (NH-95), Ferozepur-152004, India.

\*Email of the corresponding author: [amitgrover\\_321@rediffmail.com](mailto:amitgrover_321@rediffmail.com)

## Abstract

The mobile data applications has increased the demand for wireless communication systems offering high throughput, wide coverage, and improved reliability. The main challenges in the design of wireless communication systems are the limited resources, such as constrained transmission power, scarce frequency bandwidth, and limited implementation complexity—and the impairments of the wireless channels, including noise, interference, and fading effects. Multiple-Input Multiple-Output (MIMO) communication has been shown to be one of the most promising emerging wireless technologies that can efficiently boost the data transmission rate, improve system coverage, and enhance link reliability. By employing multiple antennas at transmitter and receiver sides, MIMO techniques enable a new dimension – the spatial dimension – that can be utilized in different ways to combat the impairments of wireless channels. This article focuses on Equalization techniques, for Rayleigh Flat fading channel. Equalization is a well known technique for combating intersymbol interference; moreover equalization is the filtering approach which minimizes the error between actual output and desired output by continuous updating its filter coefficients. In this paper, different equalization techniques are investigated for the analysis of BER in MIMO Systems. In this article we have discussed different types of equalizer like ZF, MMSE, ZF-SIC, MMSE-SIC, ML and Sphere decoder. The results are decoded using the ZF, MMSE, ZF-SIC, MMSE-SIC, ML and Sphere decoder (SD) technique. The successive interference methods outperform the ZF and MMSE however their complexity is higher due to iterative nature of the algorithms. ML provides the better performance in comparison to others. Sphere decoder provides the best performance and the highest decoding complexity as compare to ML. We can clearly observe that Sphere decoder gives us high performance in comparison to ML, MMSE-SC, ZF-SIC, MMSE and ZF.

**Keywords:** Quadrature Amplitude Modulation (QAM), Quadrature Phase Shift Key (QPSK), Binary Phase Shift Key (BPSK), Minimum mean-squared error (MMSE), Maximum likelihood (ML), Bit error rate (BER), Independent identical distributed (i.i.d. ), Intersymbol interference (ISI). Successive interference cancellation (SIC), Sphere Decoder (SD), zero Forcing (ZF).

## 1. Introduction

The use of multiple antennas at the transmitter and receiver in wireless systems, known as MIMO. Communication in wireless channels is impaired predominantly by multipath fading. Multipath is the arrival of the transmitted signal at the receiver through differing angles and/or differing time delays and/or differing frequency [12]. MIMO offers significant increases in data throughput and link range without additional bandwidth or transmit power. It achieves this by higher spectral efficiency and link reliability and or diversity. Because of these three properties, MIMO is an important part of modern wireless communication [10].

MIMO has multiple transmitting antennas and multiple receive antennas and, finally, MIMO-multiuser(MIMO-MU), which refers to a configuration that comprises a base station with Multiple transmit/receive antennas interacting with multiple users, each with one or more antennas. The information bits to be transmitted are encoded and interleaved[2]. The interleaved codeword is mapped to data symbols (such as bpsk ,qpsk, qam etc.) by the symbol mapper. These data symbols are input to a Space Time encoder that outputs one or more spatial data streams. .the spatial data streams are mapped to the transmit antennas by the space-time precoding block. The signals launched from the transmit antennas propagate through the channel and arrive at the receiver antenna array. The receiver collects the signals at the output of each receive antenna element and reverses the transmitter operations in order to decode the data receives space time processing, followed by space time decoding, symbol demapping, deinterleaving and decoding[8] as shown in Figure 1.

## 2.MIMO System Model

We consider a MIMO system with a transmit array of  $M_T$  antennas and a receive array of  $M_R$  antennas [5]. The block diagram of such a system is shown in Figure2. The transmitted matrix is a  $M_T \times 1$  column matrix  $s$  where  $s_i$  is the  $i$  th

component, transmitted from antenna  $i$ . We consider the channel to be a Gaussian channel such that the elements of  $s$  are considered to be independent identically distributed (i.i.d.) Gaussian variables. If the channel is unknown at the transmitter, we assume that the signals transmitted from each antenna have equal powers of  $E_s/M_T$ . The covariance matrix for this transmitted signal is given by

$$R_{ss} = \frac{E_s}{M_T} I_{M_T} \quad (1)$$

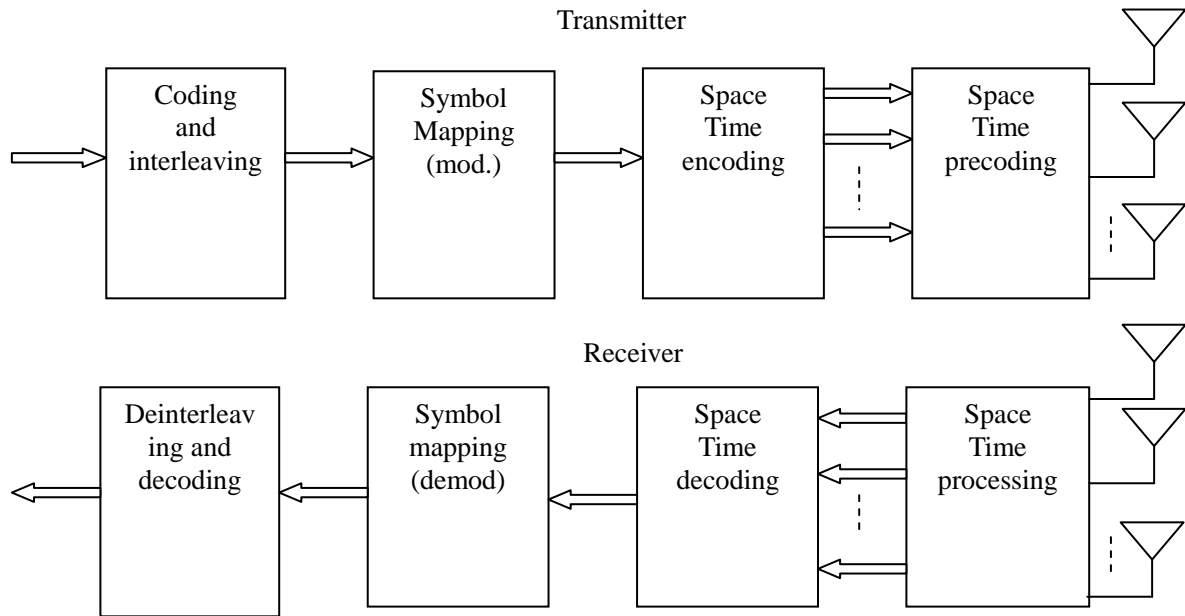


Figure1. Shows the basic building blocks that comprise a MIMO communication system.

Where  $E_s$  is the power across the transmitter irrespective of the number of antennas  $M_T$  and  $I_{M_T}$  is an identity matrix. The channel matrix  $H$  is a  $M_R \times M_T$  complex matrix. The component  $h_{i,j}$  of the matrix is the fading coefficient from the  $j$ th transmit antenna to the  $i$ th receive antenna [14]. We assume that the received power for each of the receive antennas is equal to the total transmitted power  $E_s$ . The received signals constitute a  $M_R \times 1$  column matrix denoted by  $r$ , where each complex component refers to a receive antenna. Since we assumed that the total received power per antenna is equal to the total transmitted power, the SNR can be written as

$$\gamma = \frac{E_s}{N_0} \quad (2)$$

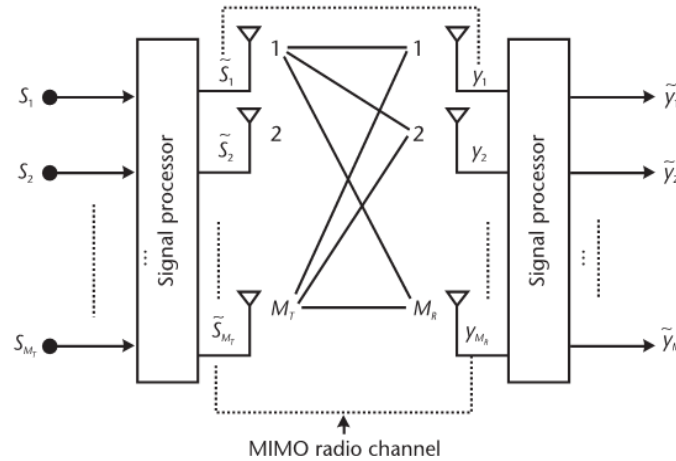


Figure2. MIMO system model

Where  $E_S$  the signal is power and  $N_0$  is the noise power.  
 Let us consider for 2 x 2 MIMO System

The received signal on the first receive antenna is

$$r_1 = h_{11}s_1 + h_{12}s_2 + n_1 \quad (3)$$

The received signal on the second receive antenna is

$$r_2 = h_{21}s_1 + h_{22}s_2 + n_2 \quad (4)$$

Where  $r_1$  and  $r_2$  are the received symbol on the first and second antenna respectively,  
 $h_{11}$  is the channel from 1<sup>st</sup> transmit antenna to 1<sup>st</sup> receive antenna,  
 $h_{12}$  is the channel from 2<sup>nd</sup> transmit antenna to 1<sup>st</sup> receive antenna,  
 $h_{21}$  is the channel from 1<sup>st</sup> transmit antenna to 2<sup>nd</sup> receive antenna,  
 $h_{22}$  is the channel from 2<sup>nd</sup> transmit antenna to 2<sup>nd</sup> receive antenna,  
 $s_1$  and  $s_2$  are the transmitted symbols and  $n_1$  and  $n_2$  is the noise on 1<sup>st</sup> and 2<sup>nd</sup> receive antennas respectively

$Eq^n$  (3) And  $Eq^n$  (4) can be represented in matrix form

$$\begin{bmatrix} r_1 \\ r_2 \end{bmatrix} = \begin{bmatrix} h_{11} & h_{12} \\ h_{21} & h_{22} \end{bmatrix} \begin{bmatrix} s_1 \\ s_2 \end{bmatrix} + \begin{bmatrix} n_1 \\ n_2 \end{bmatrix} \quad (5)$$

Therefore, the received vector can be expressed as

$$r = Hs + n \quad (6)$$

For a system with  $M_T$  transmit antennas and  $M_R$  receive antennas, the MIMO channel at a given time instant may be represented as a  $M_R \times M_T$  matrix

$$H = \begin{bmatrix} H_{1,1} & H_{1,2} & \dots & H_{1,M_T} \\ H_{2,1} & H_{2,2} & \dots & H_{2,M_T} \\ \vdots & \vdots & \ddots & \vdots \\ H_{M_R,1} & H_{M_R,2} & \dots & H_{M_R,M_T} \end{bmatrix} \quad (7)$$

### 3.MIMO Channel

#### 3.1 Classical independent, identically distributed (i.i.d.) Rayleigh fading channel model.

The degree of correlation between the individual  $M_T M_R$  channel gains comprising the MIMO channel is a complicated function of the scattering in the environment and antenna spacing at the transmitter and the receiver[8]. Consider an extreme condition where all antenna elements at the transmitter are collocated and likewise at the receiver. In this case, all the elements of H will be fully correlated (in fact identical) and the spatial diversity order of the channel is one. De-correlation between the channel elements will increase with antenna spacing. Scattering in the environment in combination with

adequate antenna spacing ensures de-correlation of the MIMO channel elements. With rich scattering, the typical antenna spacing required for de-correlation is approximately  $\lambda/2$ , where  $\lambda$  is the wavelength corresponding to the frequency of operation. Under ideal conditions when the channel elements are perfectly de-correlated, We get  $H = H_w$ , the classical i.i.d. Frequency-flat Rayleigh fading MIMO channel [32].

The channel model above assumes that the product of the bandwidth and the delay spread is very small. With increasing bandwidth and/or delay spread this product is no longer negligible, resulting in channel realizations that are frequency-dependent that is  $H(f)$ . Where fading at a given frequency may be de-correlated in the spatial domain, correlation may exist across channel elements in the frequency domain. The correlation properties in the frequency domain are a function of the power delay profile. The coherence bandwidth  $B_c$  is defined as the minimum separation in bandwidth required to achieve de-correlation. For two frequencies  $f_1$  and  $f_2$  with  $|f_1 - f_2| > B_c$ , we have

$$E[\text{vec}(H(f_1)) \text{vec}^H(H(f_2))] = 0 \quad (8)$$

The coherence bandwidth is inversely proportional to the delay spread of the channel. Due to the motion of scatters in the environment or of the transmitter or receiver, the channel realizations will vary with time. As with the case of frequency-selective fading, we can define a coherence time  $T_c$ , defined as the minimum separation in time required for de-correlation of the time-varying channel realizations [3]. For two time instances  $t_1$  and  $t_2$  with  $|t_1 - t_2| > T_c$ , we have

$$E[\text{vec}(H(t_1)) \text{vec}^H(H(t_2))] = 0 \quad (9)$$

The coherence time is the inversely proportion to the Doppler spread of the channel.

### 3.2 Real- World MIMO channel.

In practice, the behaviour of  $H$  can significantly deviate from  $H_w$  due to a combination of inadequate antenna spacing and/or inadequate scattering leading to spatial fading correlation. Furthermore, the presence of a fixed (possibly line-of-sight or LOS) component in the channel will result in Ricean fading [9].

In the presence of an LOS component between the transmitter and the receiver, the MIMO channel may be modeled as the sum of a fixed component and a fading component.

$$H = \sqrt{\frac{k}{1+k}} \bar{H} + \sqrt{\frac{k}{1+k}} H_w \quad (10)$$

are:

$\sqrt{\frac{k}{1+k}} \bar{H} = E[H]$  is the LOS component of the channel.

$\sqrt{\frac{k}{1+k}} H_w$  is the fading component.

$k \geq 0$  in equation (9) is the Ricean  $k$ -factor of the channel and is defined as ratio of the power in the LOS component of the channel to the power in the fading component. When  $k = 0$ , We have pure Rayleigh fading channel. At the other extreme  $k = \infty$  corresponds to a non-fading channel [16]. In general, real-world MIMO channels will exhibit some combination of Ricean fading and spatial fading correlation. With appropriate knowledge of the MIMO channel at the transmitter, the signalling strategy can be appropriately adapted to meet performance requirements [38]. The channel state information could be complete (i.e., the precise channel realization) or partial (i.e., knowledge of the spatial correlation,  $K$ -factor, etc.).

## 4.Equalization Techniques.

### 4.1 Zero forcing

An ISI channel may be modelled by an equivalent finite-impulse response (FIR) filter plus noise. A zero-forcing equalizer uses an inverse filter to compensate for the channel response function[23]. In other words, at the output of the equalizer, it has an overall response function equal to one for the symbol that is being detected and an overall zero response for other symbols. If possible, this results in the removal of the interference from all other symbols in the absence of the noise. Zero forcing is a linear equalization method that does not consider the effects of noise. In fact, the noise may be enhanced in the

process of eliminating the interference.

Let us assume the case that  $M_T = M_R$  and  $H$  is a full rank square matrix. In this case, the inverse of the channel matrix  $H$  exists and if we multiply both sides of equation (7) by  $H^{-1}$ , we have

$$yH^{-1} = x + nH^{-1} \quad (11)$$

From above equation we can see that symbols are separated from each other.

To solve for  $x$ , We know that we need to find a matrix  $W_{ZF}$  which satisfies  $W_{ZF} H = 1$ . The Zero forcing linear detector for meeting this constraint is given by:

$$W_{ZF} = (H^H H)^{-1} H^H \quad (12)$$

The covariance matrix of the effected noise may be calculated as:

$$E[(nH^{-1})^H \cdot nH^{-1}] = (H^{-1})^H \cdot E[n^H \cdot n] \cdot H^{-1} = n(H \cdot H^H)^{-1} \quad (13)$$

It is clear from the above equation that noise power may increase because of the factor  $(H \cdot H^H)^{-1}$ . In general if the number of transmitter and receiver antennas is not same, we may multiply by Moore–Penrose generalized inverse, pseudo-inverse of  $H$  to achieve a similar zero-forcing result.

In other words, it inverts the effect of channel as

$$\begin{aligned} \tilde{x}_{ZF} &= W_{ZF} y \\ &= x + (H^H H)^{-1} n \end{aligned} \quad (14)$$

The error performance is directly proportion connected to the power of  $(H^H H)^{-1} n$  that is  $\|(H^H H)^{-1} n\|_2^2$ .

Using SVD post- detection noise power can be evaluated as:

$$= \sum_{i=1}^{M_T} \frac{\sigma_n^2}{\sigma_i^2}$$

#### 4.2 Minimum mean square error (MMSE)

If the mean square error between the transmitted symbols and the outputs of the detected symbols, or equivalently, the received SNR is taken as the performance criteria, the MMSE detector is the optimal detection that seeks to balance between cancelation of the interference and reduction of noise enhancement.

Let us denote MMSE detector as  $W_{MMSE}$  and detection operation by

$$\hat{x}_k = \text{sgn} [W_{MMSE} y]$$

The  $W_{MMSE}$  that maximizes the SNR and minimizes the mean square error which is given by:

$$E[(\hat{x}_k - W_{MMSE} y)^T (\hat{x}_k - W_{MMSE} y)]$$

To solve for  $x$ , We know that we need to find a matrix  $W_{MMSE}$ . The MMSE linear detector for meeting this constraint is given by:

$$W_{MMSE} = (H^H H + \sigma_n^2 I)^{-1} H^H \quad (15)$$

Therefore

$$W_{MMSE} = \left( H^* H + \frac{1}{SNR} I \right)^{-1} H^* \quad (16)$$

Where

- $(H^*)$  is the complex conjugate of  $H$
- We assume that the number of receive antennas is less than the number of transmit antennas  $M \geq N$
- SNR is Signal to Noise Ratio

MMSE at a high SNR

$$W_{MMSE} = \left( H^* H + \frac{1}{SNR} I \right)^{-1} H^* \approx (H^H H)^{-1} H^H \quad (17)$$

At a high SNR MMSE becomes Zero Forcing.

### 4.3 Successive Interference Cancellation.

When signals are detected successively, the outputs of previous detectors can be used to aid the operations of next ones which leads to the decision directed detection algorithms including SIC, Parallel Interference cancellation (PIC), and multistage detection. ZF SIC with optimal ordering, and MMSE-SIC with equal power allocation approaches the capacity of the i.i.d. Rayleigh fading channel [23]. After the first bit is detected by the decorrelator the result is used to cancel the interference from the received signal vector assuming the decision of the first stream is correct [27]. For the ZF-SIC, since the interference is already nulled, the significance of SIC is to reduce the noise amplification by the nulling vector. The nulling vector  $w_1$  filters the received vector  $y$  as:

$$\hat{x}_k = \text{sgn} [ w_1^T y ] \quad (18)$$

Assuming  $\hat{x}_k = x_1$ , by substituting  $x_1$  from the received vector  $y$ , we obtain a modified received vector  $y_1$  given by:

$$y_1 = y - \hat{x}_k(H)_1 \quad (19)$$

Where  $(H)_1$  denotes the first column of  $H$ . We then repeat this operation until all  $M_T$  bits are detected. Once the first stream is detected, the first row of  $H$  is useless and will be eliminated. Therefore after the first cancellation the nulling vector for the second stream need only  $M_r - 1$  dimensions. For the MMSE detector the significance of SIC is not only to minimize the amplification of noise but also the cancellation of the interference from other antennas. In addition, there is another opportunity to improve the performance by optimal ordering the SIC process. The ordering is based on the norm of the nulling vector. At each stage of cancellation, instead of randomly selecting the stream to detect, we choose the nulling vector that has the smallest norm to detect the corresponding data stream. This scheme is proved to be the globally optimum ordering more complex.

### 4.4 Maximum Likelihood (ML)

The Linear detection method and SIC detection methods require much lower complexity than the optimal ML detection, but their performance is significantly inferior to the ML detection [24]. Maximum likelihood detection calculates the Euclidean distance between received signal vector and the product of all possible transmitted signal vectors with the given channel  $H$ , and finds the one with minimum distance. Let  $C$  and  $N_T$  denote a set of signal constellation symbol points and a number of transmit antennas, respectively. Then, ML detection determines the estimate transmitted signal vector  $x$  as:

$$\hat{x}_{ML} = \underset{x \in C^{N_T}}{\text{argmin}} \|y - Hx\|^2 \quad (20)$$

Where:

$\|y - Hx\|^2$  corresponds to the ML metric. The ML method achieves the optimal performance as the maximum a posteriori detection when all the transmitted vectors are likely. However, its complexity increases exponentially as modulation order and/or the number of transmit antennas increases [31]. The required number of ML metric calculation is  $|C|^{N_T}$ , that is the complexity of metric calculation exponentially increases with the number of antennas.

The ML receiver performs optimum vector decoding and is optimal in the sense of minimizing the error probability. ML receiver is a method that compares the received signals with all possible transmitted signal vectors which is modified by channel matrix  $H$  and estimates transmit symbol vector  $\hat{C}$  according to the Maximum Likelihood principle, which is shown as:

$$\hat{C} = \underset{c}{\text{min arg}} \|y - C'H\|_F^2 \quad (21)$$

where  $_F$  is the Frobenius norm. Expanding the cost function using Frobenius norm given by

$$\hat{C} = \underset{c}{\text{min arg}} \left[ \text{Tr}[(y - C'H)^H \cdot (y - C'H)] \right] \quad (22)$$

$$\hat{C} = \underset{c}{\text{min arg}} \left[ \text{Tr}[y^H \cdot y + H^H \cdot C'^H \cdot C' \cdot H - H^H \cdot C'^H \cdot y - y^H \cdot C' \cdot H] \right] \quad (23)$$

Considering  $r^H$ .  $r$  is independent of the transmitted codeword so can be rewritten as

$$\hat{C} = \underset{c}{\text{min arg}} \left[ \text{Tr}[H^H \cdot C'^H \cdot C' \cdot H] - 2 \cdot \text{Real}(\text{Tr}[H^H \cdot C'^H \cdot y]) \right] \quad (24)$$

where  $\cdot^H$  is a Hermitian operator. Although ML detection offers optimal error performance, it suffers from complexity issues.

#### 4.5 Sphere Decoder (SD)

The main idea behind sphere decoding is to limit the number of possible codewords by considering only those codewords that are within a sphere centered at the received signal vector. Sphere decoding method intends to find the transmitted signal vector with minimum ML metric, that is, to find the ML solution vector. However it considers only a small set of vectors within a given sphere rather than all possible transmitted signal vectors [27]. Sphere Decoder adjusts the sphere radius until there exists a single vector (ML solution vector) within a sphere.

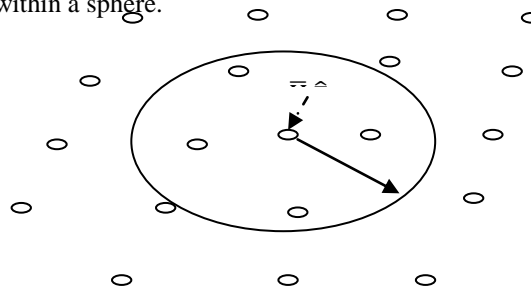


Figure4. Original Sphere in Sphere Decoder

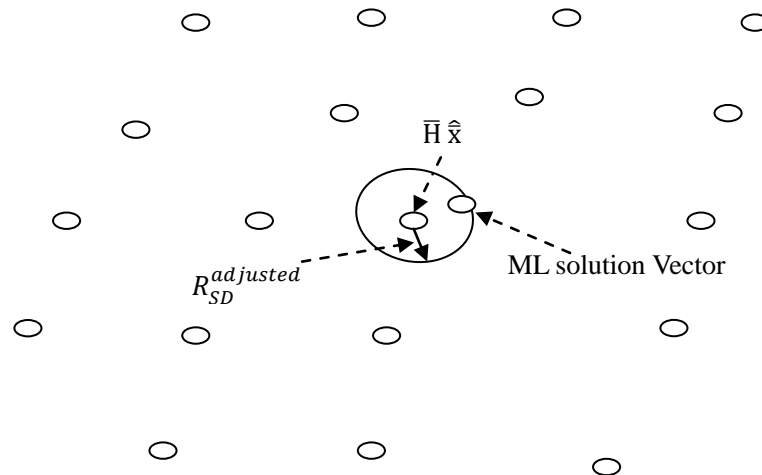


Figure5. New sphere with reduced radius.

It increases the radius when there exists no vector within a sphere, and decreases the radius when there exists multiple vectors within a sphere.

In the sequel, we sketch the idea of the SD through an example. Consider a square QAM in a  $2 \times 2$  MIMO channel. The complex system may be converted into an equivalent real system. Let  $y_{jR}$  and  $y_{jI}$  denote the real and imaginary parts of the received signal at the  $j^{\text{th}}$  receiving antenna, that is,  $y_{jR} = \text{Re}\{y_j\}$  and  $y_{jI} = \text{Im}\{y_j\}$ . Similarly, the input signal  $x_i$  from the  $i^{\text{th}}$  antenna can be represented by  $x_{iR} = \text{Re}\{x_i\}$  and  $x_{iI} = \text{Im}\{x_i\}$ .

For  $2 \times 2$  MIMO channel, the received signal can be expressed in terms of its real and imaginary parts as follows.

$$\begin{bmatrix} y_{1R} + jy_{1I} \\ y_{2R} + jy_{2I} \end{bmatrix} = \begin{bmatrix} h_{11R} + jh_{11I} & h_{12R} + jh_{12I} \\ h_{21R} + jh_{21I} & h_{22R} + jh_{22I} \end{bmatrix} \begin{bmatrix} x_{1R} + jx_{1I} \\ x_{2R} + jx_{2I} \end{bmatrix} + \begin{bmatrix} z_{1R} + jz_{1I} \\ z_{2R} + jz_{2I} \end{bmatrix} \quad (25)$$

Where  $h_{ij} = \text{Re}\{h_{ij}\}$ ,  $h_{ij} = \text{Im}\{h_{ij}\}$ ,  $z_i = \text{Re}\{z_i\}$ , and  $z_i = \text{Im}\{z_i\}$ . The real and imaginary parts of Equation (25) can be expressed as:

$$\begin{bmatrix} y_{1R} \\ y_{2R} \end{bmatrix} = \begin{bmatrix} h_{11R} & h_{12R} \\ h_{21R} & h_{22R} \end{bmatrix} \begin{bmatrix} x_{1R} \\ x_{2R} \end{bmatrix} - \begin{bmatrix} h_{11I} & h_{12I} \\ h_{21I} & h_{22I} \end{bmatrix} \begin{bmatrix} x_{1I} \\ x_{2I} \end{bmatrix} + \begin{bmatrix} z_{1R} \\ z_{2R} \end{bmatrix} \quad (26)$$

$$= \begin{bmatrix} h_{11R} & h_{12R} & -h_{11I} & -h_{12I} \\ h_{21R} & h_{22R} & -h_{21I} & -h_{22I} \end{bmatrix} \begin{bmatrix} x_{1R} \\ x_{2R} \\ x_{1I} \\ x_{2I} \end{bmatrix} + \begin{bmatrix} z_{1R} \\ z_{2R} \end{bmatrix}$$

And,

$$\begin{bmatrix} y_{1I} \\ y_{2I} \end{bmatrix} = \begin{bmatrix} h_{11I} & h_{12I} & h_{11R} & h_{12R} \\ h_{21I} & h_{22I} & h_{21R} & h_{22R} \end{bmatrix} \begin{bmatrix} x_{1R} \\ x_{2R} \\ x_{1I} \\ x_{2I} \end{bmatrix} + \begin{bmatrix} z_{1I} \\ z_{2I} \end{bmatrix} \quad (27)$$

The above two equations can be combined to yield the following expression:

$$\begin{bmatrix} y_{1R} \\ y_{2R} \\ y_{1I} \\ y_{2I} \end{bmatrix} = \begin{bmatrix} h_{11R} & h_{12R} & -h_{11I} & -h_{12I} \\ h_{21R} & h_{22R} & -h_{21I} & -h_{22I} \\ h_{11I} & h_{12I} & h_{11R} & h_{12R} \\ h_{21I} & h_{22I} & h_{21R} & h_{22R} \end{bmatrix} \begin{bmatrix} x_{1R} \\ x_{2R} \\ x_{1I} \\ x_{2I} \end{bmatrix} + \begin{bmatrix} z_{1R} \\ z_{2R} \\ z_{1I} \\ z_{2I} \end{bmatrix} \quad (28)$$

For  $\bar{y}$ ,  $\bar{H}$ ,  $\bar{x}$  and  $\bar{z}$  defined in above equation, the SD method exploits the following relation:

$$\arg \min_{\hat{x}} \|(\bar{y} - \bar{H}\hat{x})\|^2 = \arg \min_{\hat{x}} (\bar{x} - \hat{x})^T \bar{H}^T \bar{H} (\bar{x} - \hat{x}) \quad (29)$$

Where  $\hat{x} = (\bar{H}^H \bar{H})^{-1} \bar{H}^H \bar{y}$ , which is the unconstrained solution of the real system shown in Equation (28). It shows that the ML solution can be determined by different metric

$(\bar{x} - \hat{x})^T \bar{H}^T \bar{H} (\bar{x} - \hat{x})$ . Consider the following sphere with radius of  $R_{SD}$ .

$$(\bar{x} - \hat{x})^T \bar{H}^T \bar{H} (\bar{x} - \hat{x}) \leq R_{SD}^2 \quad (30)$$

The SD method considers only the vectors inside a sphere defined by Equation (30). Figure4. illustrates a sphere with the center of  $\hat{x} = (\bar{H}^H \bar{H})^{-1} \bar{H}^H \bar{y}$  and radius of  $R_{SD}$ . We are taking a example that sphere includes four candidate vectors, one of which is the ML solution vector. No vector outside the sphere can be the ML solution vector because their ML metric values are bigger than the ones inside the sphere [24]. If we were fortunate to choose the closest one among the four candidate vectors, we can reduce the radius in Equation (30) so that we may have a sphere within which a single vector remains.

In other words, the ML solution vector is now constrained in this sphere with a reduced radius, as shown in Figure5.

The new metric in Equation (29) is also expressed as.

$$(\bar{x} - \hat{x})^T \bar{H}^T \bar{H} (\bar{x} - \hat{x}) = (\bar{x} - \hat{x})^T R^T R (\bar{x} - \hat{x}) = \|R(\bar{x} - \hat{x})\|^2 \quad (31)$$

Where R is obtained from QR decomposition of the real channel matrix  $\bar{H} = QR$ . When  $N_T = N_R$ , the metric in Equation (31) is given as

$$\|R(\bar{x} - \hat{x})\|^2 = \left\| \begin{bmatrix} r_{11} & r_{12} & r_{13} & r_{14} \\ 0 & r_{22} & r_{23} & r_{24} \\ 0 & 0 & r_{33} & r_{34} \\ 0 & 0 & 0 & r_{44} \end{bmatrix} \begin{bmatrix} \bar{x}_1 - \hat{x}_1 \\ \bar{x}_2 - \hat{x}_2 \\ \bar{x}_3 - \hat{x}_3 \\ \bar{x}_4 - \hat{x}_4 \end{bmatrix} \right\|^2 \quad (32)$$

$$= |r_{44}(\bar{x}_4 - \hat{x}_4)|^2 + |r_{33}(\bar{x}_3 - \hat{x}_3)|^2 + |r_{34}(\bar{x}_4 - \hat{x}_4)|^2 + |r_{22}(\bar{x}_2 - \hat{x}_2)|^2 + |r_{23}(\bar{x}_3 - \hat{x}_3)|^2 + |r_{24}(\bar{x}_4 - \hat{x}_4)|^2 \\ + |r_{11}(\bar{x}_1 - \hat{x}_1)|^2 + |r_{12}(\bar{x}_2 - \hat{x}_2)|^2 + |r_{13}(\bar{x}_3 - \hat{x}_3)|^2 + |r_{14}(\bar{x}_4 - \hat{x}_4)|^2 \quad (33)$$

From Equation (31) and Equation (33), the sphere in Equation (30) can be expressed as

$$= |r_{44}(\bar{x}_4 - \hat{x}_4)|^2 + |r_{33}(\bar{x}_3 - \hat{x}_3)|^2 + |r_{34}(\bar{x}_4 - \hat{x}_4)|^2 + |r_{22}(\bar{x}_2 - \hat{x}_2)|^2 + |r_{23}(\bar{x}_3 - \hat{x}_3)|^2 \\ + |r_{24}(\bar{x}_4 - \hat{x}_4)|^2 + |r_{11}(\bar{x}_1 - \hat{x}_1)|^2 + |r_{12}(\bar{x}_2 - \hat{x}_2)|^2 + |r_{13}(\bar{x}_3 - \hat{x}_3)|^2 \\ + |r_{14}(\bar{x}_4 - \hat{x}_4)|^2 \leq R_{SD}^2 \quad (34)$$

Using the Sphere in Equation (34), the details of SD method are now described with the following four steps.

Step 1. Referring to Equation (34), we first consider a candidate value for  $\hat{x}_4$  in its own single dimension, that is, which is arbitrarily chosen from the points in the sphere

$$|r_{14}(\bar{x}_4 - \hat{x}_4)|^2 \leq R_{SD}^2.$$

In other words, this point must be chosen in the following range:

$$\hat{x}_4 - \frac{R_{SD}}{r_{44}} \leq \bar{x}_4 \leq \hat{x}_4 + \frac{R_{SD}}{r_{44}} \quad (35)$$

Let  $\tilde{x}_4$  denote the point chosen in step 1. If there exists no candidate point satisfying the inequalities, the radius needs to be increased. We assume that a candidate value was successfully chosen. Then we proceed to next step.

Step 2. Referring to equation Equation (34) again, a candidate value for  $\bar{x}_3$  is chosen from the points in the following sphere.

$$|r_{44}(\tilde{x}_4 - \hat{x}_4)|^2 + |r_{33}(\bar{x}_3 - \hat{x}_3)|^2 + |r_{34}(\tilde{x}_4 - \hat{x}_4)|^2 \leq R_{SD}^2 \quad (36)$$

Which is equivalent to

$$\begin{aligned} \hat{x}_3 - \frac{\sqrt{R_{SD}^2 - |r_{44}(\tilde{x}_4 - \hat{x}_4)|^2 - r_{34}(\tilde{x}_4 - \hat{x}_4)}}{r_{33}} &\leq \bar{x}_3 \\ &\leq \hat{x}_3 + \frac{\sqrt{R_{SD}^2 - |r_{44}(\tilde{x}_4 - \hat{x}_4)|^2 - r_{34}(\tilde{x}_4 - \hat{x}_4)}}{r_{33}} \end{aligned} \quad (37)$$

The  $\tilde{x}_4$  in Equation (37) is the one already chosen in Step 1. If a candidate value for  $\bar{x}_3$  does not exist, we go back to Step 1 and choose other candidate value of  $\tilde{x}_4$ . Then search for  $\bar{x}_3$  that meets the inequalities in equation (37) for given  $\tilde{x}_4$ . In case that no candidate value  $\bar{x}_3$  exists with all possible values  $\tilde{x}_4$ , we increase the radius of sphere,  $R_{SD}$ , and repeat the step 1. Let  $\tilde{x}_4$  and  $\tilde{x}_3$  denote the final points chosen from Step 1 and Step 2 respectively.

Step 3. Given  $\tilde{x}_4$  and  $\tilde{x}_3$ , a candidate value for  $\bar{x}_2$  is chosen from the points in the following sphere:

$$\begin{aligned} &= |r_{44}(\tilde{x}_4 - \hat{x}_4)|^2 + |r_{33}(\tilde{x}_3 - \hat{x}_3)|^2 + |r_{34}(\tilde{x}_4 - \hat{x}_4)|^2 + |r_{22}(\bar{x}_2 - \hat{x}_2)|^2 + |r_{23}(\tilde{x}_3 - \hat{x}_3)|^2 \\ &\quad + |r_{24}(\tilde{x}_4 - \hat{x}_4)|^2 \leq R_{SD}^2 \end{aligned} \quad (38)$$

Arbitrary value is chosen for  $\bar{x}_2$  inside the sphere of Equation (38). In choosing a point, the inequality in Equation (38) is used as in the previous steps. If no candidate value of  $\bar{x}_2$  exists, we go back to Step 2 and choose another candidate value  $\tilde{x}_3$ . In case that no candidate value for  $\bar{x}_2$  exists after trying all possible candidate value for  $\tilde{x}_3$ , we go back to Step 1 and choose another candidate value for  $\tilde{x}_4$ .

The final points chosen from Step 1 through step 3 are denoted as  $\tilde{x}_4$ ,  $\tilde{x}_3$  and  $\tilde{x}_2$ , respectively.

Step 4. Now a candidate value for  $\bar{x}_1$  is chosen from the points in the following sphere:

$$\begin{aligned} &= |r_{44}(\tilde{x}_4 - \hat{x}_4)|^2 + |r_{33}(\tilde{x}_3 - \hat{x}_3)|^2 + |r_{34}(\tilde{x}_4 - \hat{x}_4)|^2 + |r_{22}(\bar{x}_2 - \hat{x}_2)|^2 + |r_{23}(\tilde{x}_3 - \hat{x}_3)|^2 \\ &\quad + |r_{24}(\tilde{x}_4 - \hat{x}_4)|^2 + |r_{11}(\bar{x}_1 - \hat{x}_1)|^2 + |r_{12}(\bar{x}_2 - \hat{x}_2)|^2 + |r_{13}(\tilde{x}_3 - \hat{x}_3)|^2 \\ &\quad + |r_{14}(\tilde{x}_4 - \hat{x}_4)|^2 \leq R_{SD}^2 \end{aligned} \quad (39)$$

An arbitrary value satisfying Equation (39) is chosen for  $\bar{x}_1$ . If no candidate value for  $\bar{x}_1$  exists, we go back to Step 3 to choose other candidate value for  $\tilde{x}_2$ . In case that no candidate value for  $\bar{x}_1$  exists after trying all possible candidate value for  $\tilde{x}_2$ , we go back to step 2 to choose another value for  $\tilde{x}_3$ . Let  $\tilde{x}_1$  denote the candidate value for  $\bar{x}_1$ . Once we find all candidate values,  $\tilde{x}_4$ ,  $\tilde{x}_3$ ,  $\tilde{x}_2$  and  $\tilde{x}_1$ , then corresponding radius is calculated by using Equation (39) Using new radius Step 1 is repeated. If  $[\tilde{x}_1 \tilde{x}_2 \tilde{x}_3 \tilde{x}_4]$  turns out to be a single point inside a sphere with that radius, it is declared as the ML solution vector and searching procedure stops.

The main advantage of using sphere decoder over ML is that the complexity is significantly reduced. The complexity of sphere decoder depends on how well the initial radius is chosen.

## 5. Simulation and Results

The MATLAB script perform the transmission of different binary sequences (two symbols in one time slot) after modulating

these using different modulation techniques like bpsk, qpsk and 16 QAM, multiply the symbol with the channel and then add white Gaussian noise and perform the equalization on the received signal using different equalizers and then demodulate these using the multiple values of SNR and plot the simulation results. These different simulation results are shown below in the different graphs, which provide the comparison of the BER for different modulation techniques using different equalizers like MMSE, ZF, ZF-SIC, MMSE-SIC and ML with Rayleigh flat fading channel.

**Comparison of BER for different modulations with MMSE equalizer in 2x2 MIMO systems with Rayleigh flat fading channel**  
**and Comparison of BER for different modulations with ZF equalizer in 2x2 MIMO systems with Rayleigh flat fading channel.**

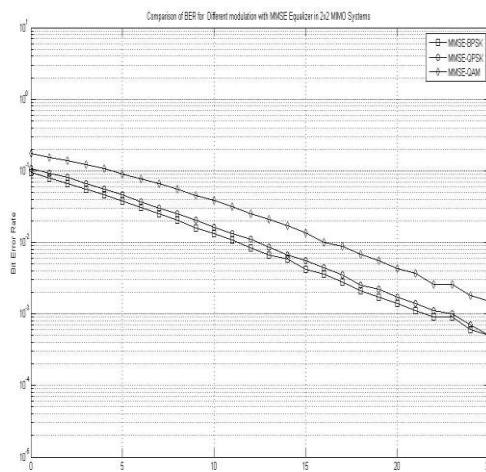


**Figure6.**

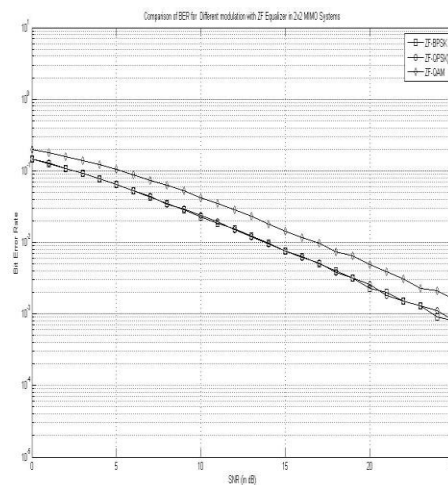


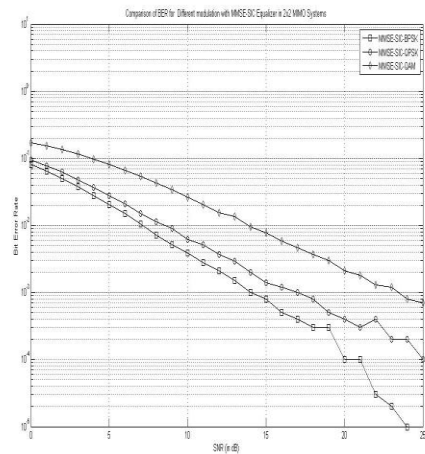
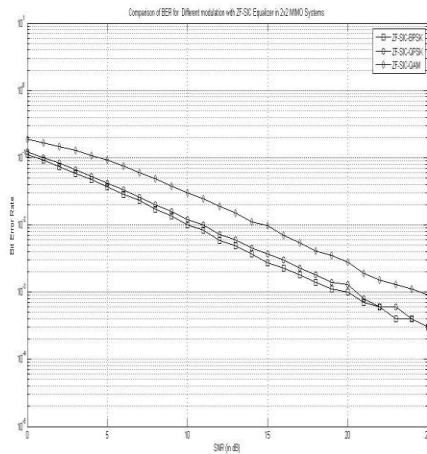
**Figure7.**

It has been observed from the figure.6 that with the BPSK modulation we get the best result in comparison to 16 QAM whereas the result from BPSK and QPSK are almost same. So the order of performance in decreasing order is MMSE–BPSK > MMSE-QPSK > MMSE-16 QAM and from the figure.7, that with the BPSK modulation, we get the best result in comparison to 16 QAM whereas the result from BPSK and QPSK are almost same. So the order of performance in decreasing order is ZF – BPSK > ZF-QPSK > ZF-16 QAM.

**Comparison of BER for different modulations with ZF-SIC equalizer in 2x2 MIMO systems with Rayleigh flat fading channel**

**Figure8.**

**Figure9.**



From figure.8, it has been observed that the BER performance of ZF-SIC is better and with the BPSK modulation we get the best result in comparison to 16 QAM whereas the result from BPSK and QPSK are almost same. So the order of performance in decreasing order is ZF-SIC– BPSK > ZF-SIC -QPSK > ZF-SIC-16 QAM. From figure.9, we observe that the BER performance of MMSE-SIC is better than previous discussed equalizers and with the BPSK modulation we get the best result in comparison to 16 QAM whereas the result from BPSK and QPSK are almost same. So the order of performance in decreasing order is MMSE-SIC– BPSK > MMSE-SIC -QPSK > MMSE-SIC-16 QAM.

**Comparison of BER for different modulations with ML equalizer in 2x2 MIMO systems with Rayleigh flat fading channel and Comparison of BER for BPSK with different equalizers in 2X2 MIMO Systems in Rayleigh flat fading channel.**

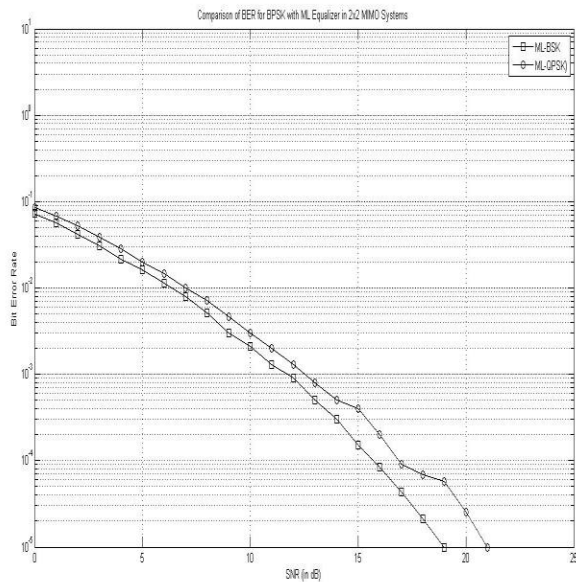


**Figure10.**

In figure.10, we have observed that the BER performance of ML is better than previous discussed equalizers. It is also observed that the complexity of ML equalizer increases with as we go to BPSK to QPSK and with the BPSK modulation we get the best result in comparison to QPSK. So the order of performance in decreasing order is ML- BPSK > ML – QPSK. Figure11 shows the simulation results for transmitting 2 bits/sec over two transmit and two receive antennas using BPSK. The results are decoded using the ZF, MMSE, ZF-SIC, MMSE-SIC, ML and Sphere decoder (SD) technique. The linear equalizers (ZF, MMSE and ML) perform worse than other methods while requiring a lower complexity. The

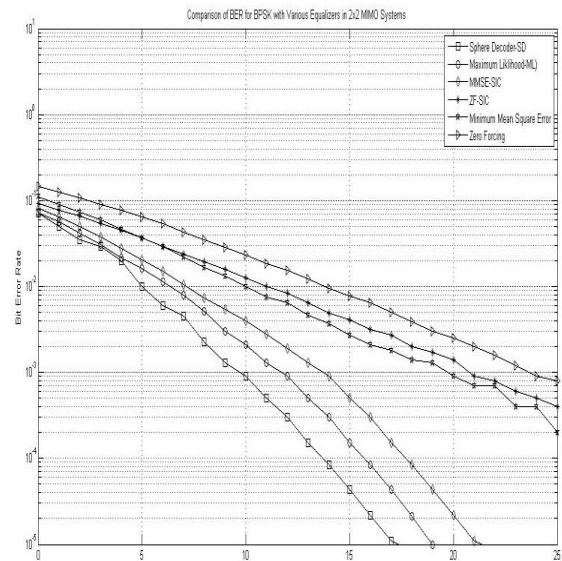


**Figure11.**

---

successive interference methods outperform the ZF and MMSE however their complexity is higher due to iterative nature of the algorithms. ML provides the better performance in comparison to all previously discussed. Sphere decoder provides the best performance and the highest decoding complexity as compare to ML.

### **Conclusions**

We have applied different equalizers to Rayleigh flat fading channel, the performance of SD is better than all the other equalizers. Performance of ML is also better than other equalizers but if we look at the complexity term then Sphere decoder is less complex than ML. The complexity of ML decoder goes on increasing as we move to higher modulation schemes, whereas complexity in SD depends on how well the initial radius is chosen.

### **Future Scope**

For further improvement of the BER performance of the MIMO system, we can use Blind equalization, which is a digital processing technique and the transmitted signal is equalized from the received signal while making use only of the transmitted signal statistics. Blind equalization is essentially blind de-convolution applied to the digital communication. Array processing decoders can also be used for getting high BER performance.

## References

- [1]. H. El Gamal and A.R. Hammons (2001), "The layered space-time architecture: a new perspective", *IEEE Trans. Inform. Theory*, vol. 47, pp. 2321–2334, Sept. 2001.
- [2]. Simon, M. K. and Alouini (2004), *M. Digital Communication over Fading Channels*. John Wiley & Sons, 2004.
- [3]. G.J. Foschini and M.J. Gans (1998), "On limits of wireless communications in a fading environment when using multiple antennas", *Wireless Personal Communications*, vol. 6, 1998, pp. 311–335.
- [4]. G.J. Foschini (1996), "Layered space-time architecture for wireless communications in a fading environment when using multiple antennas", *Bell Labs.Tech.J.*, vol. 6, no. 2, pp. 41–59, 1996.
- [5]. V. K. Garg and J.E. Wilkes (1996), *Wireless and Personal Communications Systems*, Prentice Hall, 1996.
- [6]. J. C. Liberti and T. S. Rappaport (1999), *Smart Antennas for Wireless Communications*, Prentice H all PTR, 1999.
- [7]. J. G. Proakis, *Digital Communications*, McGraw-Hill series in electrical and computer engineering, 1995.
- [8]. G. J. Foschini and M. J. Gans (1998), "On limits of wireless communications in a fading environment when using multiple antennas", *Wireless Personal Communications*, Mar. 1998, pp. 311–335.
- [9]. H. El Gamal and R. Hammons (2001), "A new approach to layered space-time coding and signals processing", *IEEE Trans. Inform. Theory*, vol. 47, no. 6, Sept. 2001, pp. 2321–2334.
- [10]. D. Gesbert (2003), "MIMO space-time coded wireless systems," presentation, Sept. 2003, available at <http://www.tele.ntnu.no/projects/beats/course.htm>.
- [11]. G. D. Golden, G. J. Foschini, R. A. Valenzuela and P. W. Wolniansky (1999), "Detection algorithm and initial laboratory results using the V-BLAST space-time communication architecture", *Electronics Letters*, vol. 35, no. 1, Jan. 7, pp. 14–15.
- [12]. D. Shiu and J. M. Kahn (1999), "Layered space-time codes for wireless communications using multiple transmit antennas," *ICC'99*, Vancouver, Canada.
- [13]. G. Foschini, G. G olden, R. Valenzuela and P. Wolniansky (2000), "Simplified processing for high spectral efficiency wireless communication employing multi-element arrays", *IEEE Journal on Selected Areas in Communications*, vol. 17, pp. 1841–1852.
- [14]. D. Wubben, R. Bohnke, J. Rinas, V. Kuhn and K .D. Kammeyer (2001), "Efficient algorithm for decoding layered s pace-time codes", *Electronics Letters*, vol. 37, pp. 1348–1350.
- [15]. K.Lo, S.Marinkovic, Z C hen and B.Vucetic (2002), "BER performance comparison of layered space time codes", *ICC 2002*, New York, USA.
- [16]. D. Shiu and J. M. Kahn (1999), "Layered space-time codes for wireless communications using multiple transmit antennas," *ICC'99*, Vancouver, Canada.
- [17]. D. N. C. Tse L. Zheng (2003), "Diversity and multiplexing: a fundamental trade-off in multiple antenna channels," *IEEE Trans. Inform. Theory*, vol. 49, no. 5, pp. 1073–1096.
- [18]. R. A. Valenzuela G. D. Golden, C. J. Foschini and P. W. Wolniansky (1999), "Detection algorithm and initial laboratory results using V-BLAST space-time communication architecture," *Electronics Lett.*, vol. 35, no. 1.
- [19]. G. J. Foschini (1996), "Layered space-time architecture for wireless communication in a fading environment using multi-element antennas," *Bell-Labs Techn. J.*, pp. 41–59.
- [20]. R. U. Nabar A. J. Paulraj, D. A. Gore and H. Bolcskei (2004), "An overview of MIMO communications—a key to gigabit wireless," *Proceedings of the IEEE*, vol. 92, no. 2, pp. 198–218.

- [21]. Choo, Y. S., Kim, J., Yang, W. Y., and Kang, C. G. MIMO-OFDM Wireless Communication with MATLAB. IEEE Press, John Wiley and Sons (Asia) Pte Ltd.
- [22]. Ezio Biglieri, Robert Calderbank, Anthony Constantinides, Andrea Goldsmith, Arogyaswami Paulraj, H. Vincent Poor (2007), "MIMO Wireless Communications", Cambridge University Press.
- [23]. G. Arslan, B. L. Evans, and S. Kiaei (2000), "Equalization for Discrete Multitone Receivers To Maximize Channel Capacity", IEEE Transactions on Signal Processing, submitted March 30.
- [24]. J. Zhang, T. Bhatt, G. Mandyam (2003), "Efficient linear equalization for high data rate downlink CDMA signaling", 37th IEEE Asilomar Conference on Signals, Systems and Computers.
- [25]. D. Shiu, P. J. Smith, D. Gesbert, M. Shafi and A. Nayguib (2003), "From theory to practice: An overview of MIMO space-time coded wireless systems," IEEE J. Select. Areas Commun. vol. 21, no. 3, pp. 281–302.
- [26]. C. E. Proakis, "Digital Communications," McGraw-Hill International Editions, New York, 4th edition, 2000.
- [27]. Wang and G. B. Giannakis (2003), "A simple and general parametrization quantifying performance in fading channels," IEEE Trans. Commun., vol. 51, no. 8, pp. 1389–1398.
- [28]. H. Jafarkhani (2005), "Space-time coding: Theory & Practice", Cambridge University Press.
- [29]. R. U. Nabar, A. J. Paulraj, D. A. Gore and H. Bolcskei, "An overview of MIMO communications—a key to gigabit wireless," Proceedings of the IEEE, vol. 92, no. 2, pp. 198–218.
- [30]. M. Janakiraman (2004), "Space-time codes and MIMO systems", Artech House.
- [31]. I. E. Telatar (1999), "Capacity of multi-antenna Gaussian channels," European Transactions on Telecommunications, vol. 10, no. 6, pp. 585–595.
- [32]. G. Foschini (1996), "Layered space-time architecture for wireless communication in a fading environment when using multiple antennas," Bell Labs, Technical Journal 2, appeared in Volume 1, number 2, pp 41–59.
- [33]. G. D. Golden, G. J. Foschini, R. A. Valenzuela, and P. W. Wolniansky (1999), "Detection algorithm and initial laboratory results using the V-BLAST space-time communication architecture," Electron Lett., vol. 35, no. 1, pp. 1415.
- [34]. G. Ginis and J. M. Cioffi (2001), "On the relationship between V-BLAST and GDFE," IEEE Communications Letters, vol. 5, pp. 364–366.
- [35]. S. Loyka and F. Gagon (2004), "Performance analysis of the V-BLAST algorithm: an analytical approach," IEEE Transactions on Wireless Communications. Vol. 3, pp. 1326–1337, July 2004.
- [36]. L. Zheng and D. Tse (2003), "Diversity and multiplexing: A fundamental trade-off in multiple-antenna channels," IEEE Transactions on Information Theory, vol. 49, pp. 1073–1096, May 2003.
- [37]. K. I. Pedersen, J. B. Anderson, J. P. Kermoal and P. E. Mogensen (2000), "A stochastic multiple-input multiple-output radio channel model for evaluation of space-time coding algorithms," in Proc. VTC 2000 Fall, Boston, vol. 2, pp. 893–897, Sep. 2000.
- [38]. M. Varanasi and T. Guess (1997), "Optimum decision feedback multiuser equalization with successive decoding achieves the total capacity of the Gaussian multiple-access channel," Conference Record of the Thirty-First Asilomar Conference on signals, Systems and computers, vol. 2, pp. 1405–1409, Nov-2-5 1997.
- [39]. A. M. Tulino and S. Verdú (2004), Random Matrix Theory and Wireless Communications. Hanover, MA 02339, USA: now publishers Inc., 2004.
- [40]. E. Biglieri, J. Proakis and S. Shamai (1998), "Fading Channel: Information Theoretic and Communication Aspects", IEEE Trans. On information Theory, Vol. 44, pp. 2619–2692, Oct. 1998.
- [41]. X. Li, H. Huang, G. J. Foschini, and R. A. Valenzuela (2000), "Effects of Iterative Detection and Decoding on the Performance of BLAST", IEEE Global Telecommunications Conference, vol. 2, pp. 1061–10066, Nov 2000.

- [42]. David Tse and Pramod Viswanath, Fundamentals of Wireless Communication, Cambridge University Press, 2005.
- [43]. G.J.Foschini (1996), "Layered space-time architecture for wireless communication in a fading environment when using multielement antennas," BLTJ, Autumn, 1996.
- [44]. G. D. Golden , G. J. Foschini, R. A. Valenzuela and P. W. Wolniansky (1999), " Detection algorithm and initial laboratory results using v-blast space-time communication architecture," IEE Electronic Letters, Vol.35, No.1, pp.14~16, 7th January 1999.
- [45]. John G. Proakis and Masoud Salehi (2000), "Contemporary Communication Systems using Matlab," Brooks/Cole, 2000



**Rohit gupta** received his B.Tech degree in Electronics and Communication Engineering in 2011 from Chitkara Institute of Engineering and Technology, Rajpura, Punjab, India. At present, He is Pursuing his Master's in Electronics and Communication Engineering from Shaheed Bhagat Singh State Technical Campus, Ferozepur, Punjab, India.



**Amit Grover (M'06-SM'09-PI'11&12 )** The author became a Member (M) of Association ISTE in 2006, a Senior Member (SM) of society SELCOME in september 2009, and a Project-Incharge (PI) in august 2011 and in September 2012. The author place of birth is Ferozepur, Punjab, India on 27<sup>th</sup>, September 1980.The author received M.Tech degree in Electronics and Communication Engineering from Punjab Technical University, Kapurthla, Punjab, India in 2008 and received B.Tech degree in Electronics and Communication Engineering from Punjab Technical University, Kapurthala, Punjab, India in 2001. Currently, he is working as an Assistant Professor in Shaheed Bhagat Singh State Technical Campus, Ferozpur, Punjab. His area of interest includes signal processing, mimo systems, wireless mobile communication, and high speed digital communications and 4G wireless communications.

This academic article was published by The International Institute for Science, Technology and Education (IISTE). The IISTE is a pioneer in the Open Access Publishing service based in the U.S. and Europe. The aim of the institute is Accelerating Global Knowledge Sharing.

More information about the publisher can be found in the IISTE's homepage:

<http://www.iiste.org>

## CALL FOR PAPERS

The IISTE is currently hosting more than 30 peer-reviewed academic journals and collaborating with academic institutions around the world. There's no deadline for submission. **Prospective authors of IISTE journals can find the submission instruction on the following page:** <http://www.iiste.org/Journals/>

The IISTE editorial team promises to review and publish all the qualified submissions in a **fast** manner. All the journals articles are available online to the readers all over the world without financial, legal, or technical barriers other than those inseparable from gaining access to the internet itself. Printed version of the journals is also available upon request of readers and authors.

### IISTE Knowledge Sharing Partners

EBSCO, Index Copernicus, Ulrich's Periodicals Directory, JournalTOCS, PKP Open Archives Harvester, Bielefeld Academic Search Engine, Elektronische Zeitschriftenbibliothek EZB, Open J-Gate, OCLC WorldCat, Universe Digital Library, NewJour, Google Scholar

